Teknik Dergi, 2022 12553-12576, Paper 694

Modification in Response of a Bridge Seismically Isolated with Lead Rubber Bearings Exposed to Low Temperature

Esengul CAVDAR[1]
Volkan KARUK[2]
Gokhan OZDEMIR[3]

ABSTRACT

This study investigates the response modification in a bridge seismically isolated with lead rubber bearings (LRBs), due to change of ambient temperature from 20ºC to -30ºC. Accordingly, a large-size LRB was tested after being conditioned at corresponding temperatures and changes in its hysteretic properties were noted. Use of analytical tool in modeling nonlinear response of the tested LRB was justified by comparing the experimentally observed and analytically obtained force-displacement curves. Then, verified analytical representation of an LRB was employed in nonlinear response history analyses conducted to quantify the change in response of a representative LRB isolated bridge when subjected to bidirectional ground motion excitations at 20°C and -30°C. Analyses results are also employed to assess the use of property modification factor, λ, to change isolator properties in order to represent low temperature behavior. It is revealed that for the selected ground motion records, the average isolator force remains almost the same for both ambient temperatures. Moreover, using property modification factor will result in accurately estimated isolator displacements, but overestimated isolator forces, in an average sense.

Keywords: Seismic isolation, lead rubber bearing, low temperature, lead core heating, bridge.

Note:
- This paper was received on February 16, 2021 and accepted for publication by the Editorial Board on August 13, 2021.
- Discussions on this paper will be accepted by November 30, 2022.
- https://doi.org/10.18400/tekderg.880787

1 Eskisehir Technical University, ESQUAKE Seismic Isolator Test Laboratory, Eskisehir, Turkey
esengulcavdar@eskisehir.edu.tr - https://orcid.org/0000-0003-1497-0908

2 Eskisehir Technical University, ESQUAKE Seismic Isolator Test Laboratory, Eskisehir, Turkey
volkankaruk@eskisehir.edu.tr - https://orcid.org/0000-0002-6782-7972

3 Eskisehir Technical University, ESQUAKE Seismic Isolator Test Laboratory, Eskisehir, Turkey
gokhan_ozdemir@eskisehir.edu.tr - https://orcid.org/0000-0002-2962-2327

1. INTRODUCTION

Seismic isolation is an earthquake resistant design strategy which is adopted to protect structures against adverse effects of ground motions. It relies on lengthening of natural period of structures by introducing systems that possess low horizontal stiffness between the superstructure and substructure. Accordingly, in case of a seismic excitation, rather than the seismically isolated structure, seismic isolators will undergo large deformations and dissipate energy. Among various seismic isolation systems, lead rubber bearings (LRB) are among the most widely used seismic isolators. They are composed of alternate layers of rubber and steel plates with a lead core at the center that passes through the height of the bearing. Rubber layers are responsible for the lateral stiffness of the bearing whereas lead core provides the required lateral strength. Since they were invented by Robinson in the 1970s, LRBs have been used in several structures (bridges, hospitals, data centers etc.) around the world [1-3]. In parallel, several research programs have been conducted to determine performance of LRBs under the effect of different parameters [4-10]. One of these parameters is the change in ambient temperature.

Mechanical properties of LRBs, mainly post yield stiffness and characteristic strength, are related to properties of rubber and lead, respectively. Although there are numerous studies that focused on the change in rigidity of rubber at low temperatures [11-17], very few experimental data are available for modification of LRB properties at low temperatures [18-20]. The LRB tested by Hasegawa et al. [18] was 250 mm in diameter with a lead core diameter of 38 mm. Displacement controlled LRB tests were conducted at temperatures of 40, 20, 0 and -20°C for a shear strain of 100% at 0.3 Hz. It was reported that the exposure time of the bearing to these temperatures is 5 hours. Similarly, Constantinou et al. [7] conducted tests with an LRB having rubber and lead core diameters of 381 mm and 70 mm, respectively. Isolator tests were carried out at a shear strain of 58% and loading frequency was 0.35 Hz. Constantinou et al. [7] stated that LRB was conditioned at -26°C and 20°C for 48 hours prior to tests. Compared to LRBs used in experimental studies of Hasegawa et al. [18] and Constantinou et al. [7], LRB tested by Cho et al. [19] was a large size bearing with rubber and lead core diameters of 860 mm and 170 mm, respectively. The total rubber thickness was 288 mm and tested at a shear strain of 15%. Temperatures considered by Cho et al. [19] were -20, -10, 0 and 23°C. It is to be mentioned that 15% shear strain is very low to be representative of seismic behavior of an LRB designed to undergo large deformations. Accordingly, variation in mechanical properties of a large size LRB exposed to low temperature was revisited by Park et al. [20]. Rubber and lead core diameters of the LRB were 800 mm and 180 mm, respectively and tested at a shear strain of 100%. All of the studies cited above reported that both characteristic strength and post yield stiffness of the isolator increase due to reduction in ambient temperature. Moreover, characteristic strength was observed to be more sensitive to change in ambient temperature by having large amount of increments compared to post yield stiffness.

The studies discussed so far specifically were interested in cyclic tests of LRBs exposed to different temperatures and reported solely the variations in stiffness and strength of bearings on a comparable manner based on displacement controlled test results. In recent studies, seismic performance of bridges, isolated by LRBs, under the effects of both ground motion excitations and low temperature have also been investigated. For instance, Billah and Todorov [21] examined the seismic response of an LRB isolated bridge in case of subfreezing

temperature. The authors performed nonlinear response history analyses (NRHA) using a bridge model subjected to different ground motions representative of earthquakes in Eastern Canada. In their study, LRBs were modeled with two different non-deteriorating bilinear force-displacement curves to idealize hysteretic behavior of LRBs at "summer" (25°C) and "winter" (-30°C) with properties provided by manufacturer. Another study that has focused on seismic response of LRB isolated bridge under low temperatures was conducted by Deng et al. [22]. Similarly, in the analytical model, they used a non-deteriorating hysteretic representation for LRBs where stiffness and strength of LRB was modified in accordance with an empirical formulation. LRB properties used in the analyses were computed for temperatures changing from -30°C to 40°C. However, it must be mentioned that both Billah and Todorov [21] and Deng et al. [22] neglected the deterioration in strength of LRBs due to temperature rise in the lead core under cyclic motion. Thus, those results are based on bounding analyses where hysteretic properties such as strength and stiffness of LRB do not change during the applied motion. On the other hand, it is well documented that considering the actual response (deteriorating force-displacement curve) of LRBs under cyclic motion may result in substantially different response quantities compared to analyses performed with non-deteriorating idealizations of LRBs [23-28]. In this sense, study of Wang et al. [29] presents valuable data related to performance of LRBs under ground motion excitations at low temperatures. In their research, gradual reduction in strength of isolator has been taken into account by employing the proposal of Kalpakidis et al. [30-31] for modeling of LRBs. These authors considered two different LRBs in the analytical model that can be classified as small- and moderate-size. Modeling of both LRBs was based on property modification factors proposed by Constantinou et al. [7] and Li et al. [32] rather than experimental data. From this point of view, study of Wang et al. [29] is in lack of discussion related to suitability of using these factors, which are sensitive to geometry of LRB, manufacturer of the bearing, loading protocol (shear strain and frequency) and exposure time to low temperature.

Literature review related to experimental studies show that LRBs are classified as small- to moderate-size with diameters ranging between 250 mm and 860 mm. However, the use of large-size LRBs with diameters greater than 1000 mm gets widespread interest, and the validity of available test data for such large bearings needs to be questioned. Besides, analytical studies mostly address the use of empirical formulations for modification of LRB properties rather than employing the related test data of the analyzed isolators. Furthermore, analytical representation of LRBs was performed by non-deteriorating force-displacement curves by neglecting the actual strength deterioration. Thus, there is a need to perform complementary research, composed of both experimental and analytical phases, to investigate the response of LRB isolated bridges exposed to low temperatures. The objectives of this study are (i) to determine the variation in seismic performance of an LRB isolated bridge considering their modified mechanical properties when exposed to low temperatures and (ii) to evaluate the effectiveness of property modification factors (suggested for low temperatures) employed in bounding analysis of seismically isolated structures. For this purpose, first, a large-size LRB was tested after it was conditioned at both room (20°C) and low (-30°C) temperatures under dynamic conditions. Change in the mechanical properties of this LRB will be reported. Then, the experimental data is used to verify the success of analytical model employed to idealize hysteretic response of LRBs. Accordingly, deteriorating hysteretic behavior of the LRB obtained from both experiments and analytical models were compared. Once the use of analytical model to idealize nonlinear hysteretic

behavior of LRBs has been shown to be appropriate for both conditions, a representative bridge isolated with LRBs, will be analyzed under the effect of both near-field and large-magnitude small-distance ground motions. In the analyses, both horizontal components of selected ground motions were subjected to structural model simultaneously. Finally, analyses were repeated for the same bridge model where LRBs are modelled by non-deteriorating force-displacement relations constructed by using property modification factors suggested to modify isolator characteristics in order to represent low ambient temperature. Results are presented in a comparative manner to assess the validity of evaluated response modification factors. Maximum isolator displacements (MIDs) and maximum isolator forces (MIFs) were the response quantities used to quantify the variation in seismic performance of LRB isolated bridge exposed to low temperature.

2. LRB TESTS

The bearing tested in this study is a large-size LRB with rubber and lead core diameters of 1020 mm and 190 mm, respectively. Height of the bearing is 436 mm including the top and bottom plates together with the end shim at the top. It is composed of 28 layers of rubber each of which has 10 mm thickness with a total rubber height of 280 mm. Geometrical properties of the tested LRB are presented in Figure 1.

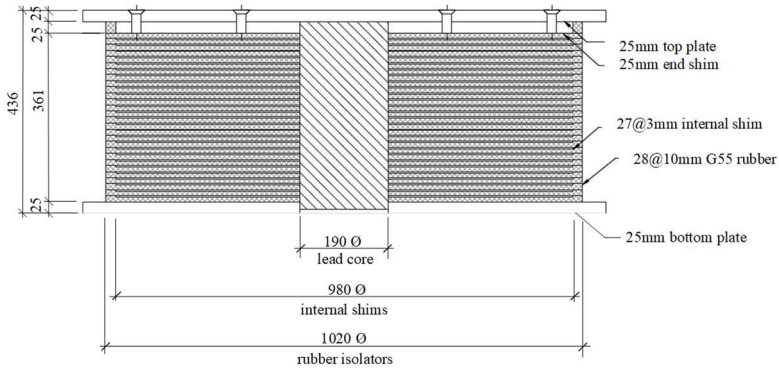

Figure 1- Section cut of test specimen (all units are in mm)

In order to determine the mechanical properties of the specimen, its hysteretic response in shear was recorded under a constant compressive load. Accordingly, the LRB was subjected to three cycles of sinusoidal motion with amplitude equal to 280 mm that corresponds to 100% shear strain. Frequency of the motion was 0.1 Hz where the maximum velocity is 176 mm/s. The axial force acting on the bearing was 4500 kN which results in 6 MPa normal stress. The LRB was first tested at a room temperature of 20°C after conditioning for 24 hours inside the laboratory and tested again at room temperature after conditioning at -30°C for 24 hours inside the air conditioned room (Figure 2.a). Selection of -30ºC with an exposure time of 24 hrs is based on the study of Guay and Bouaanani [33] where the authors focused on the low temperature exposure for design of elastomeric bridge bearings in Canada. They investigated the number of consecutive days that the ambient temperature remains below a

specific value. The authors showed that the frequency of -30 ºC for 24 hrs is in the order of 1 %. Any exposure time longer than 24 hrs was found to have almost zero frequency. This is why 24 hrs of exposure to -30 ºC is considered in the present study. Tests were conducted at ESQUAKE Seismic Isolator Test Laboratory of Eskişehir Technical University where air conditioned room and test setup are facilitated next to each other. As a result, the time spent to initiate the isolator test after conditioning is less than 10 min. Application of 4500 kN vertical force took 45 s with a loading rate of 100 kN/s. Thus, the isolator test was completed within 12 min. (10 min. + 45 s + 30 s for 3 cycles of motion with 0.1 Hz) after conditioning. The test setup of ESQUAKE shown in Figure 2.b is capable of applying dynamic motions in both horizontal and vertical directions. Table 1 presents the loading capacities of ESQUAKE test setup. Horizontal force-displacement curves obtained from tests for 20°C and -30°C are given in Figure 3.

(a) (b)

Figure 2 - (a) Air-conditioned room and (b) seismic isolator test setup of ESQUAKE

Table 1 - Properties of ESQUAKE test setup.

Max. Vertical Load:	20.000 kN
Max. Horizontal Load:	2.000 kN
Max. Horizontal Stroke:	±600 mm
Max. Velocity:	1.000 mm/s

Mechanical properties of the tested LRB such as post-yield stiffness (K_d) and characteristic strength (Q_d) for temperatures of 20°C and -30°C are presented in Table 2. Data given in Table 2 are computed by means of Eqns. (1)-(2) and Figure 4. In Eqns. (1) and (2), Q_1', Q_1'', Q_2' and Q_2'' are the isolator forces at 50% of the maximum positive and negative horizontal displacements d_{max} and d_{min} as per ISO 22762-1 [34]. Q_1 and Q_2 are the isolator forces at d_{max} and d_{min}, respectively (see Figure 4).

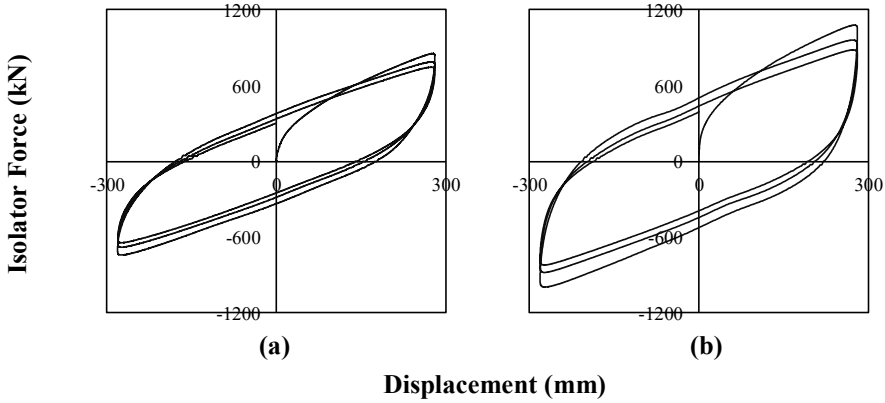

Figure 3 - Force-displacement curves of LRB tested at a) 20°C and b) -30°C.

Table 2 - Mechanical properties of LRB at 20°C and -30°C

Exposure Temperature	Cycle	Q_d (kN)	K_d (kN/m)
-30°C	1	489	2020
	2	414	1919
	3	372	1864
20°C	1	324	1833
	2	286	1796
	3	260	1766

$$Q_d = \left[\frac{Q_1'' d_{max}/2 - Q_1' d_{min}/2}{(d_{max} - d_{min})/2} - \frac{Q_2' d_{max}/2 - Q_2'' d_{min}/2}{(d_{max} - d_{min})/2} \right] / 2 \quad (1)$$

$$K_d = \left[\frac{Q_1' - Q_1''}{(d_{max} - d_{min})/2} + \frac{Q_2'' - Q_2'}{(d_{max} - d_{min})/2} \right] / 2 \quad (2)$$

Comparison of test results obtained for temperatures of 20°C and -30°C reveals the following conclusions. Characteristic strength (force intercept at zero displacement) Q_d of the tested LRB increases when the exposure temperature drops to -30°C. The amount of increase in Q_d is 50% for the first cycle whereas it is 45% and 43% for the second and third cycles, respectively. Similarly, post-yield stiffness K_d of the LRB increases as the temperature decreases. However, the amount of variations in K_d, which are 10%, 7% and 5% for first, second and third cycles, respectively, are relatively small compared to those computed for Q_d. Considering the test results, it is evident that amount of variation in mechanical properties of LRB is not constant at all loading cycles and the trend is to decrease with increasing

number of cycles. The reason for such reduction is the temperature rise in the lead core of LRB during cyclic motion as discussed in the next section.

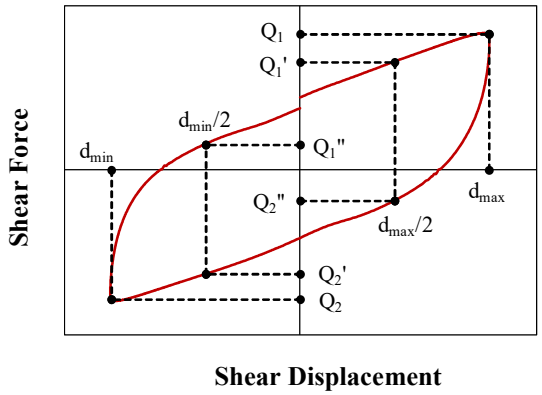

Figure 4 - Force-displacement definitions for LRBs.

3. DETERIORATING HYSTERETIC RESPONSE OF LRB

The hysteretic behavior of isolators is generally modeled by a generic non-deteriorating force-deformation relation. However, as shown in Figure 3, force-displacement curve of LRBs deteriorates under cyclic motion. Figure 3 clearly demonstrates the gradual reduction in strength of the tested bearing at each cycle. The primary reason of such a variation in strength of LRBs has been identified as the temperature rise in the lead core during cyclic motion by Kalpakidis and Constantinou [30]. Their mathematical model enables one to modify the initial strength of lead as a function of lead core temperature. Accordingly, the horizontal strength of the LRB decreases gradually when subjected to motion. The model considers the instantaneous temperature rise in the lead core and allows calculating the reduction in strength of isolator via reducing the initial yield stress of the lead (σ_{YL0}), instantly. According to this model, the relation between the lead core temperature T_L and the strength of lead (σ_{YL0}) is defined by Eqn. (3) where E_2 is a constant that relates the temperature and yield stress and equals to 0.0069/°C. For detailed information about deteriorating hysteretic response of an LRB, reference is made to Kalpakidis and Constantinou [30].

$$\sigma_{YL}(T_L) = \sigma_{YL0} \exp\left(-E_2 T_L\right) \tag{3}$$

For the sake of completeness and refraining queries regarding the analytical representation of the tested LRB in this study, Figure 5 is presented. In Figure 5, force-displacement curves obtained from experiments are compared with the analytical ones computed by means of the mathematical model proposed by Kalpakidis and Constantinou [30] for both 20°C and -30°C. OpenSees [35] is the structural analysis program by which the computations were performed. It is to be noted that the deteriorating cyclic behavior of LRB addressed in analytical modeling requires the definition of an initial yield stress for lead which is equal to the characteristic strength obtained from corresponding test result divided by the cross-sectional

area of the lead core. For detailed information about analytical modeling of LRB in OpenSees, please refer to Kumar et al. [27]. Figure 5 shows that hysteretic response of the tested LRB can be idealized realistically with great success in the analyses regardless of the ambient temperature.

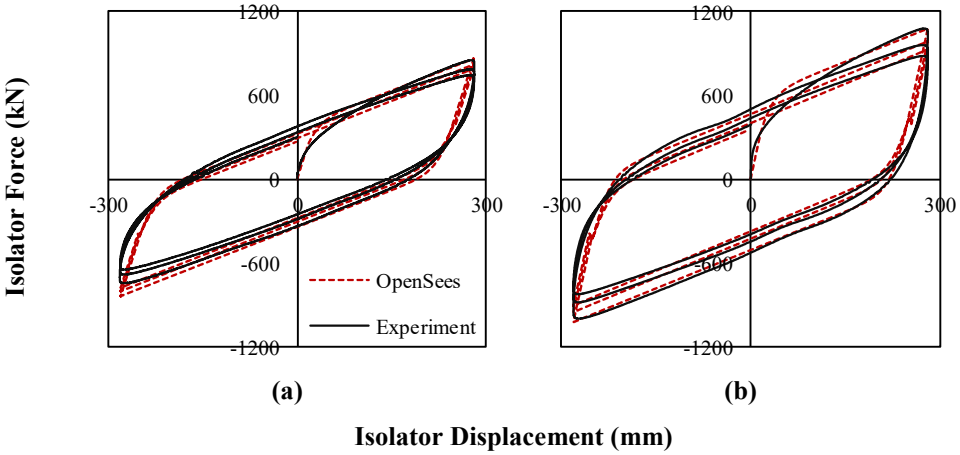

Figure 5 - Comparison of experimental and analytical hysteretic curves of LRB tested at a)20°C and b)-30°C.

4. SEISMICALLY ISOLATED BRIDGE MODEL

The analyzed bridge was originally not seismically isolated and designed for U.S. Department of Transportation Federal Highway Administration seismic design course [36]. Then, it was slightly modified (diaphragms in the box girder were added at both abutments and piers) by Constantinou et al. [7] in order to facilitate seismic isolation units between each pier/abutment and the box girder. It is a cast-in-place concrete box girder bridge with a 30-degree skew. The length of the bridge is 97.5m and has three spans with lengths of 30.5m, 36.5m and 30.5m. Intermediate bents consist of two 1.22m circular columns and a cap beam with dimensions of 1.22mx1.83m. The total weight of the bridge above the isolation level is 24956 kN (box girder and each diaphragm weigh 229 kN/m and 657 kN, respectively). The section at one of the intermediate bents is presented in Figure 6.a.

As shown in Figure 6.a, isolation system is composed of two LRBs at each abutment and pier with a total of eight isolators. They are modeled by deteriorating hysteretic behavior described in the previous section. Nonlinear bidirectional interaction of LRBs in case of simultaneous excitations of ground motions in both horizontal directions is defined in the following section. The bridge superstructure was assumed to have infinite in-plane rigidity [37-38]. Analytical representation of the bridge bent is given in Figure 6.b where $M_{superstructure}$ is defined based on the tributary weight of the superstructure plus the additional weight of the diaphragm and equals to 8330 kN (isolation period based on the post-yield stiffness of the tested LRB at 20°C is 3 s). Total mass of the bent components, M_{bent}, is lumped equally at the column tops. In the analytical model, member rigid end zone segment is taken into account to represent the bent stiffness properly. The bridge superstructure and columns are

modeled as elastic based on the assumption that structure remains within the elastic range due to seismic isolation by means of *elasticbeamcolumn* element of OpenSees [35]. Accordingly, the elastic modulus of concrete is taken as 24 820 MPa. Bridge structure is assumed to be fixed at the foundation level.

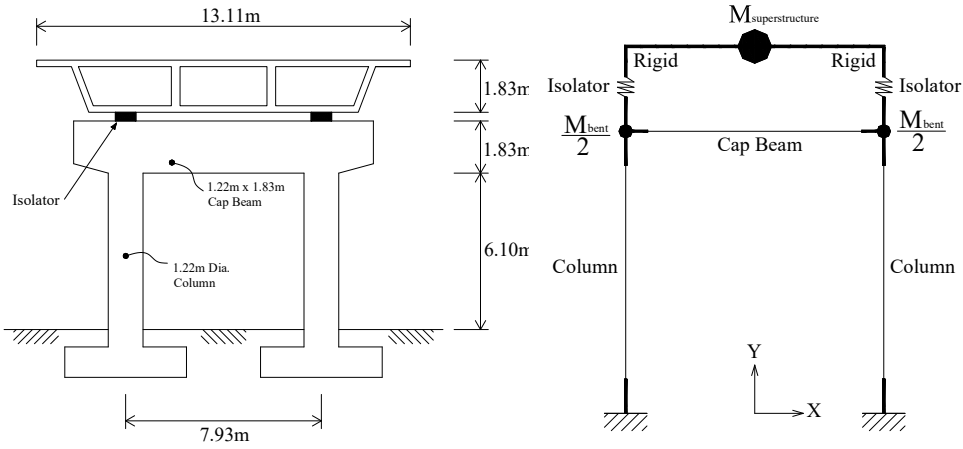

Figure 6 - (a) Bent geometry and (b) analytical model of the bent. Reprinted from [39]

5. BIDIRECTIONAL RESPONSE OF LRBS

The bidirectional bilinear hysteretic model used for modeling of LRBs was developed by Park et al. [40]. Validity of the model for idealizing the hysteretic response of isolators subjected to bidirectional ground motion excitations was tested and verified by Mokha et al. [41]. Analytical model proposed by Park et al. [40] enables assembling the isolator forces by taking into account the bidirectional interaction effects when isolators behave nonlinearly in both of the horizontal directions. Accordingly, isolator forces are calculated by Eqns. (4)-(6). By means of the off-diagonal terms of Eqn. (6), the interaction between the isolator forces in two orthogonal horizontal directions are taken into account.

$$\begin{Bmatrix} F_x \\ F_y \end{Bmatrix} = c_d \begin{Bmatrix} \dot{U}_x \\ \dot{U}_y \end{Bmatrix} + K \begin{Bmatrix} U_x \\ U_y \end{Bmatrix} + \left(\sigma_{YL}\left(T_L\right) A_L\right) \begin{Bmatrix} Z_x \\ Z_y \end{Bmatrix} \tag{4}$$

$$Y \begin{Bmatrix} \dot{Z}_x \\ \dot{Z}_y \end{Bmatrix} = \left(A[I] - B[\Omega]\right) \begin{Bmatrix} \dot{U}_x \\ \dot{U}_y \end{Bmatrix} \tag{5}$$

$$[\Omega] = \begin{Bmatrix} Z_x^2\left[\operatorname{sgn}\left(\dot{U}_x Z_x\right)+1\right] & Z_x Z_y\left[\operatorname{sgn}\left(\left(\dot{U}_y Z_y\right)+1\right)\right] \\ Z_x Z_y\left[\operatorname{sgn}\left(\left(\dot{U}_x Z_x\right)+1\right)\right] & Z_y^2\left[\operatorname{sgn}\left(\dot{U}_y Z_y\right)+1\right] \end{Bmatrix} \tag{6}$$

In the above equations, F_x and F_y are the isolator forces and U_x and U_y are the isolator displacements in x and y directions, respectively. Y and K are the yield displacement and post-yield stiffness of the bilinear force-deformation relation of isolators, respectively. c_d stands for the energy dissipation of the rubber and A_L is the cross-sectional area of the lead core. Z_x and Z_y are hysteretic dimensionless quantities that account for the interaction of hysteretic seismic isolator forces in orthogonal horizontal directions and vary between +1 and -1. In Eqn. (5), A and B values should satisfy the relation of $A = 2B$ [41] in order to assure that the force and displacement vectors are in the same direction (specifically, A=1 and B=0.5). Additionally, [I] is the unit matrix, *sgn* stands for the signum function and overdot refers to differentiation with respect to time.

6. GROUND MOTIONS

Two sets of ground motions previously used by Warn and Whittaker [37], were considered in the analyses. Each ground motion set is composed of 10 pairs of records. They were clustered to represent characteristics of near-field (NF) and large-magnitude small-distance (LMSD) records. These motions were used so that analyses results represent a broad range of seismic demand in terms of maximum isolator displacement.

Table 3 - Characteristics of selected near-field ground motions.

#	Event	Station	M_w	Comp.[1]	PGA (g)	PGV (cm/s)	PGD (cm)	Distance[2] (km)
1	Tabas, Iran	Tabas	7.4	FN	0.90	109.7	55.5	1.2
				FP	0.98	105.8	74.9	
2	Loma, Prieta	Lex Dam	7.0	FN	0.69	178.7	56.6	6.3
				FP	0.37	68.7	25.4	
3	Cape Mendocino	Petrolia	7.1	FN	0.64	62.9	14.1	8.5
				FP	0.65	46.5	10.3	
4	Erzincan, Turkey	Erzincan	6.7	FN	0.43	119.1	42.1	2.0
				FP	0.46	58.1	29.5	
5	Landers	Lucerne	7.3	FN	0.71	136.1	11.2	1.1
				FP	0.80	70.3	184.3	
6	Northridge	Rinaldi	6.7	FN	0.89	174.2	38.3	7.5
				FP	0.39	60.9	17.3	
7	Northridge	Olive View	6.7	FN	0.73	122.1	30.7	6.4
				FP	0.60	53.9	9.1	
8	Kobe	JMA	6.9	FN	1.09	160.2	40.1	3.4
				FP	0.57	72.4	15.9	
9	Chi-Chi, Taiwan	TCU065	7.	West	0.81	126.2	92.6	1.0
				North	0.60	78.8	60.8	
10	Chi-Chi, Taiwan	TCU075	7.6	West	0.33	88.3	86.5	1.5
				North	0.26	38.2	33.2	

The magnitudes of ground motions grouped as near-field are in between 6.7 and 7.6 with closest distances to the fault rupture less than 10 km. Large-magnitude small-distance ground motions have magnitudes greater than 6.5 while closest distances to fault rupture are in between 10 km and 30 km. Tables 3 and 4 give the characteristics of the considered ground motions where PGA, PGV and PGD stands for peak ground acceleration, peak ground velocity and peak ground displacement, respectively. Selected ground motions were downloaded from both the Pacific Earthquake Engineering Research (PEER) Center [42] database and library of QuakeManager [43] software. 5% damped response spectra of ground motions listed in Tables 3 and 4 are given in Figure 7 where the "strong" and "weak" components are designated based on PGVs of ground motions. The horizontal component with the larger PGV is denoted as strong component [39].

Table 4 - Characteristics of selected large-magnitude small-distance ground motions.

#	Event	Station	M_w	Comp.	PGA (g)	PGV (cm/s)	PGD (cm)	Distance[2] (km)
1	Loma Prieta	Gilroy Array #1	6.9	0	0.41	31.6	6.4	11.2
				90	0.47	33.9	8.5	
2	Kocaeli, Turkey	Gebze	7.4	0	0.24	50.3	42.8	17.0
				270	0.14	29.7	27.6	
3	Loma Prieta	Saratoga Aloha Ave	6.9	0	0.51	41.2	16.3	13.0
				90	0.32	42.6	27.6	
4	Cape Mendocino	Rio Dell Over Pass FF	7.1	270	0.39	43.8	21.7	18.5
				360	0.55	41.9	19.5	
5	Landers	Joshua Tree	7.3	0	0.27	27.5	9.5	11.6
				90	0.28	43.1	14.3	
6	Loma Prieta	Gilroy Array #2	6.9	0	0.37	32.9	7.2	12.7
				90	0.32	39.1	12.1	
7	Landers	Yermo Fire Station	7.3	270	0.25	51.4	43.9	24.9
				360	0.15	29.7	24.6	
8	Kobe	Abeno	6.9	0	0.22	20.7	9.1	23.8
				90	0.24	24.2	10.0	
9	Duzce, Turkey	Bolu	7.1	0	0.73	56.4	23.1	17.6
				90	0.82	62.1	13.6	
10	Northridge	Canoga Park Topanga Can	6.7	106	0.36	32.1	9.1	15.8
				196	0.42	60.7	20.3	

[1] FN – Fault Normal, FP – Fault Parallel

[2] Closest distance to fault rupture

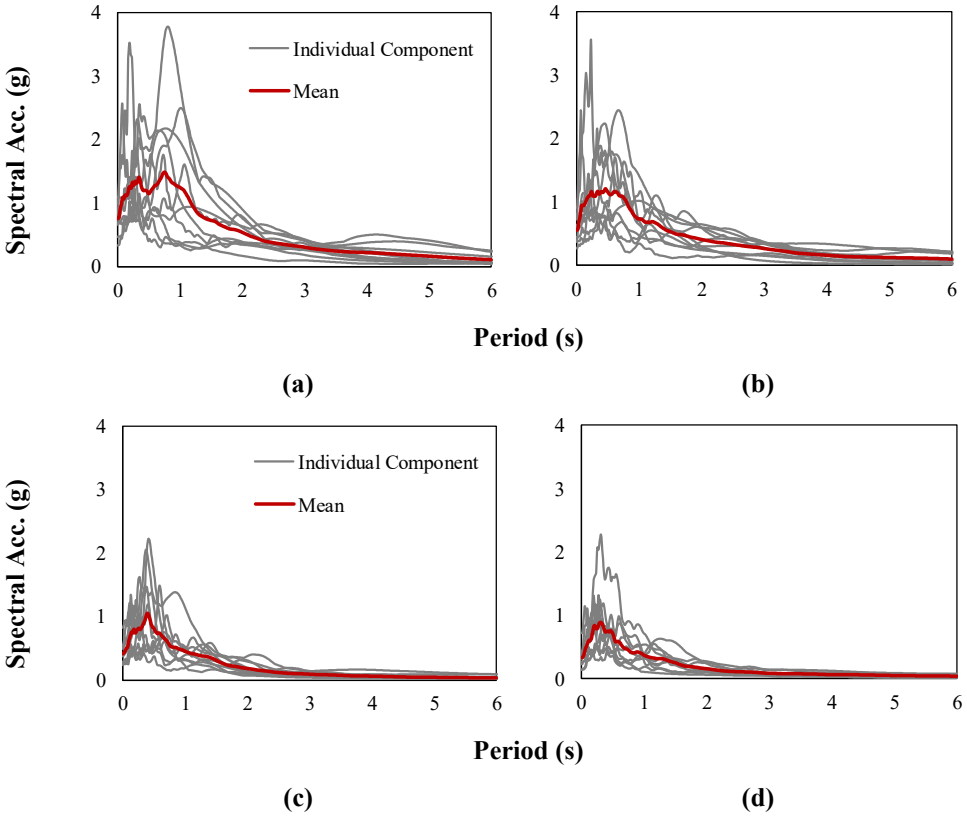

Figure 7 - 5% damped response spectra for (a) strong and (b) weak components of NF ground motions, (c) strong and (d) weak components of LMSD ground motions.

7. DYNAMIC ANALYSIS RESULTS

Nonlinear response history analyses were performed in OpenSees [35] with due consideration of deteriorating hysteretic representation of LRBs under bidirectional excitations of ground motions given Tables 3 and 4 in order to evaluate the variation in response quantities of the SIB due to change in environmental temperature. Accordingly, maximum isolator displacements (MIDs) and base shears in the pier are presented in a comparative manner for 20°C and -30°C. Moreover, the effect of seismicity level in combination with the change of environmental temperature is discussed based on analyses results obtained by using both NF and LMSD ground motion records.

7.1. Maximum Isolator Displacements

One of the important predictions for a seismically isolated bridge is the resultant displacement of the isolation system. It dominates the design of the isolator geometry together with the peak shear force transferred to the pier columns. This section presents the

observations related to variation of MID of the analyzed structural system due to change in ambient temperature. Figure 8 shows the comparison of MIDs obtained for 20°C and -30°C for both ground motion sets of NF and LMSD. Averages of MIDs recorded for all of the considered ground motion records are also given in Figure 8 where MIDs were calculated by taking the maxima of $\sqrt{\left(D_x^2 + D_y^2\right)}$. Here, D_x and D_y are the isolator displacements in horizontal x- and y-directions, respectively. Figure 8.a, where MIDs for NF ground motions are presented, reveals that MID reduces significantly when the ambient temperature drops from 20°C to -30°C. The amount of reductions in MID ranges from 8% to 53% with an average value of 19%. Similar comparison for LMSD ground motions is given in Figure 8.b. In this case, the amounts of change in MIDs for individual ground motion records range from 33% to -52% with an average of -16% when the temperature changes from 20°C to -30°C. At the end of analyses, the corresponding temperature rises in the lead core of the LRB are computed by means of the formulations proposed by Kalpakidis and Constantinou [30] for both ground motion sets and presented in Figure 9.

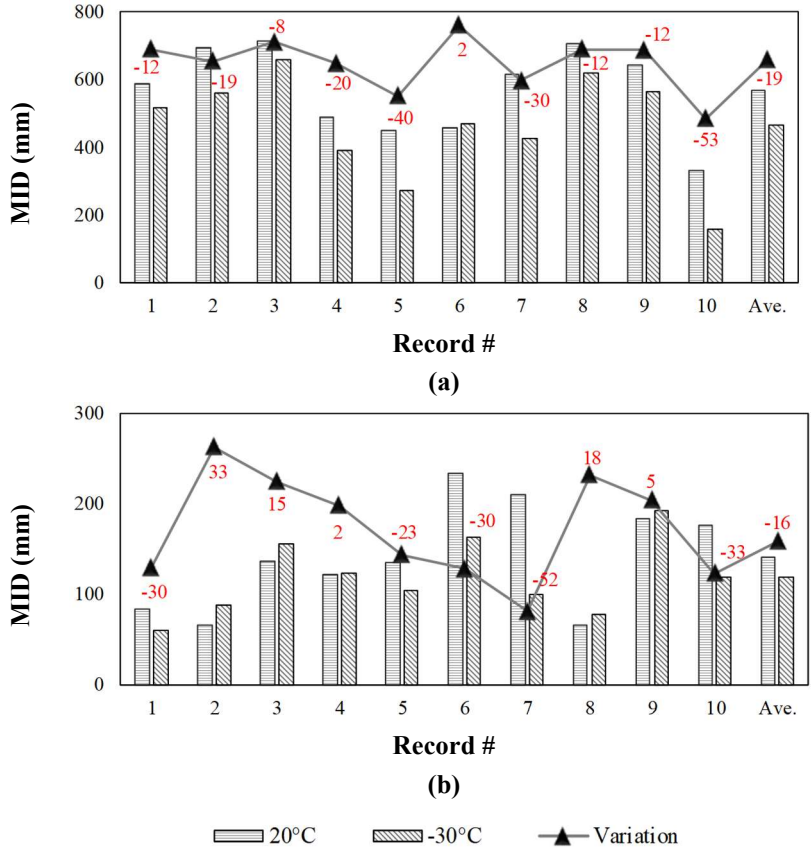

Figure 8 - Comparison of MIDs for (a) NF and (b) LMSD ground motions at 20°C and -30°C.

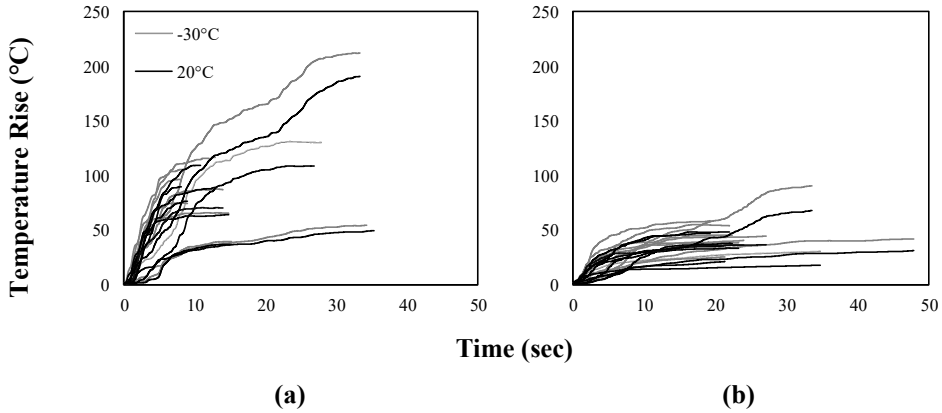

Figure 9 - Temperature rises in lead core for (a) NF and (b) LMSD ground motions at temperatures of 20°C and -30°C.

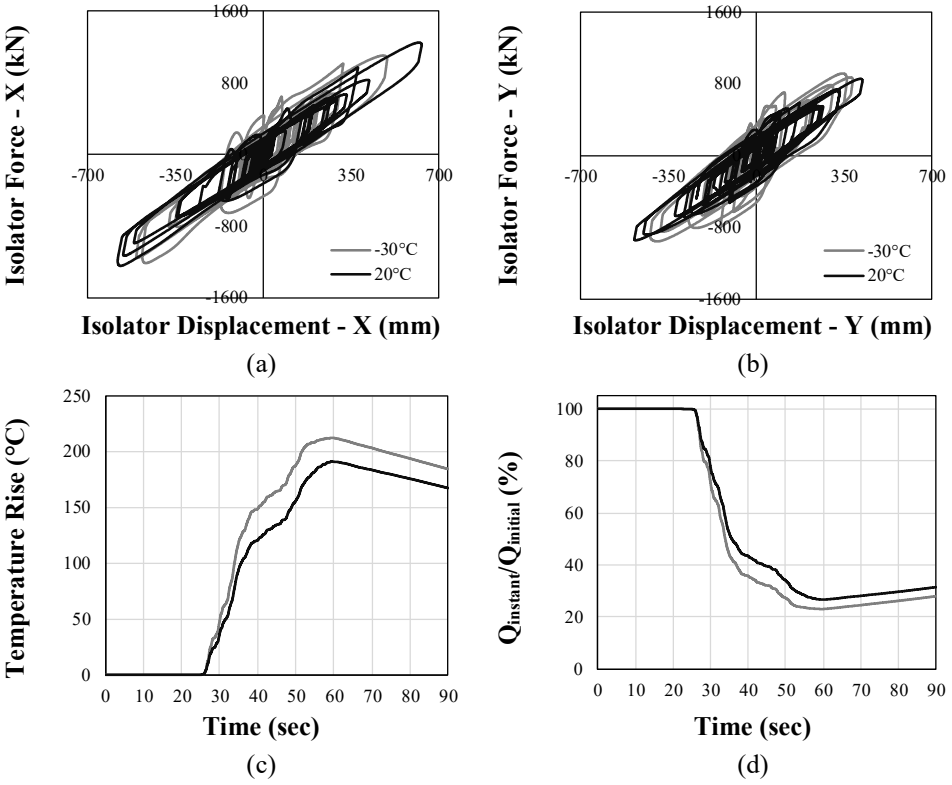

Figure 10 - (a) force-displacement curve in x-direction, (b) force-displacement curve in y-direction, (c) rise in lead core temperature, (d) change in strength of LRB for NF record #9 at 20°C and -30°C.

Since amplitudes of displacements that the LRB undergoes are larger for NF ground motions compared to LMSD ones, temperature rises in the lead core are greater for NF motions. In order to highlight the significance of strength deterioration in LRB during the analyses, Figure 10 shows force-displacement curves of the LRB for NF record #9 which has the peak value of temperature rise in Figure 9.a. Figure 10 also presents temperature rise in the lead core of the analyzed LRB and corresponding change in strength of the bearing. It is observed that the amount of temperature rise in the lead core is larger at low temperature. For record #9, maximum lead core temperatures were calculated as 213°C and 191°C for ambient temperatures of -30°C and 20°C, respectively (Figure 10.c). The corresponding losses in the initial strength of the LRB are 77% and 73%, in the same order (Figure 10.d). The reason for such high temperature rises in the lead core is the large amplitude displacement at several cycles.

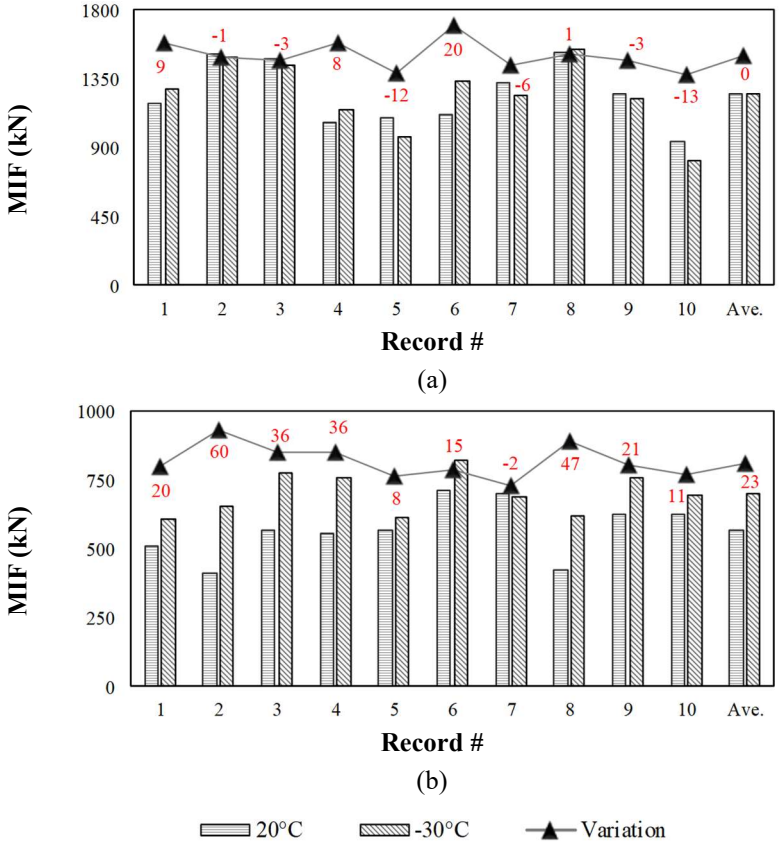

Figure 11 - Comparison of MIFs for (a) NF and (b) LMSD ground motions at 20°C and -30°C.

7.2. Base Shears in the Piers

It is of crucial importance in both performance-based design and performance assessment of a seismically isolated bridge to estimate the shear force transferred from isolation system to the piers. In this section, variation of base shear forces acting on each column of the bridge (see Figure 6) is presented in Figure 11 as a function of ambient temperature and seismicity level. For near field ground motions, Figure 11.a shows that the amounts of variation in isolator force are in between -13% to 20% when temperature decreases from 20ºC to -30ºC. However, it is interesting to observe that when the averages of base shears are of concern, they are identical for both 20ºC to -30ºC with a magnitude of 1248 kN. Although the initial strength and stiffness of isolator increases due to reduced ambient temperature, the average shear force does not change for both 20ºC to -30ºC. Even though initial strength and stiffness of the bearing increases at -30ºC due to reduced isolator displacements (compared to 20ºC case) the maximum shear force transferred by the isolator remain the same in an average sense (see Figure 10.a).

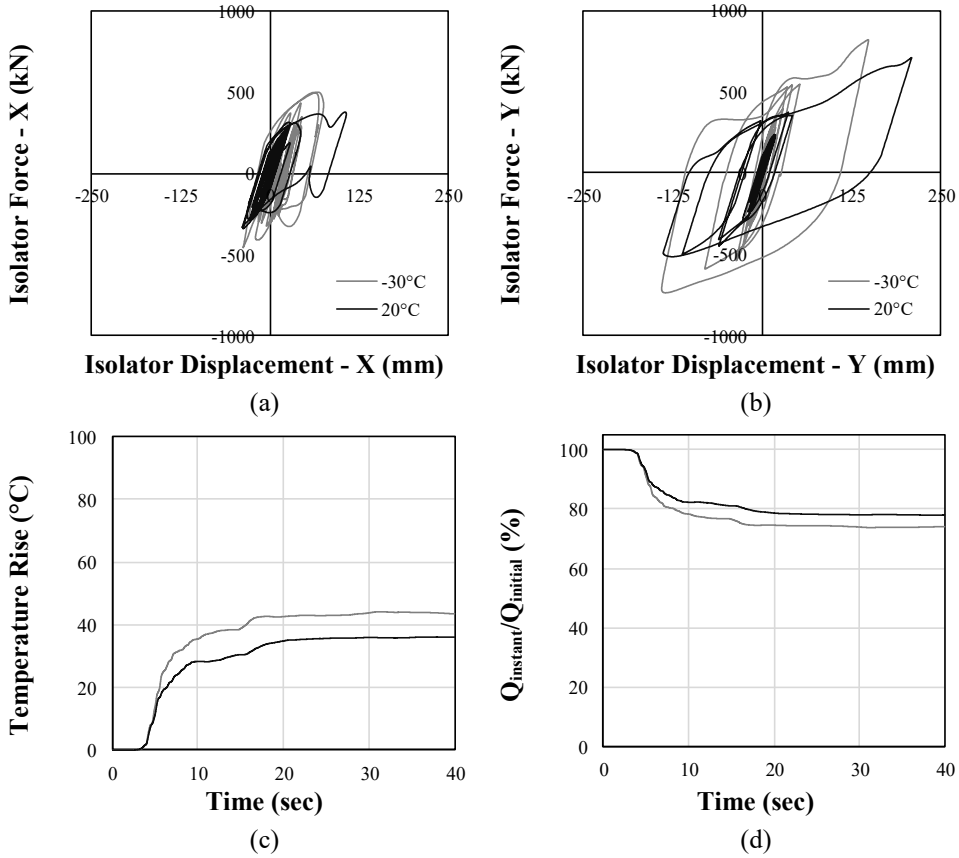

Figure 12 - (a) force-displacement curve in x-direction, (b) force-displacement curve in y-direction, (c) rise in lead core temperature, (d) change in strength of LRB for LMSD record #6 at 20°C and -30°C.

Figure 11.b is shown to investigate the variation of isolator force for large-magnitude small-distance ground motion set when the ambient temperature is reduced from 20ºC to -30ºC. Figure 11.b reveals that although the average value of amplification in isolator force is calculated as 23%, for the selected ground motions it may be up to 60%, individually. In order to understand better the change in hysteretic behavior of LRB, Figure 12 is presented for record #6 of LMSD ground motion set. As clearly shown in Figures 12.a and 12.b, the isolator undergoes a larger displacement for 20ºC compared to the30ºC case. However, isolator displacement is not large enough to overcome the isolator force recorded for -30ºC scenario where the initial strength and stiffness values are greater than those of 20ºC case. Since the isolator displacements are small, computed temperature rises in the lead core are relatively low and equal to 36ºC and 43ºC (Figure 12.c) and corresponding amounts of loss in initial strengths are 22% and 26% (Figure 12.d) for ambient temperatures of 20°C and -30°C, respectively.

8. ASSESSMENT OF USING PROPERTY MODIFICATION FACTOR

The current design approach for modeling the hysteretic behavior of seismic isolators is to perform bounding analyses. It assures that the nominal properties (defined as the average among the three cycles of force-displacement curve obtained at normal temperature) of the isolator is modified to consider the effects of aging, contamination, ambient temperature, history of loading and heating during cyclic motion. For this purpose, corresponding property modification factors, λ, are employed as defined by the design guidelines [44]. Modified properties of the isolator are used to construct non-deteriorating force-displacement curves that will represent both upper and lower bound characteristics of LRB in NRHA. Such modeling approach aims to estimate the boundaries where the probable isolator response will take place in between, rather than focusing on the real performance of the isolator. Once property modification factors are determined, it will be possible for the designer to consider the envelope response of seismically isolated structure where maximum and minimum isolator properties are established. Although it is suggested to determine the property modification factors based on test results which are specific to isolator under investigation, in the literature there are some default values used in bounding analysis. This section is devoted to assessing the validity of using the available default values of property modification factors, suggested to represent change in ambient temperature, to estimate critical response quantities of a seismically isolated structure, namely maximum isolator displacement and maximum isolator force. In this sense, property modification factors suggested by three different investigationss to mimic the change in LRB properties at low temperatures are considered and listed in Table 5. It is to be noted that, these values are specific only to isolators tested by the researchers at an ambient temperature of -30ºC. The manufacturer, size of bearing, shear modulus of rubber, exposure time to low temperature and loading frequency of the studies cited in Table 5 are all different from each other. As a result, there is a diversity in the suggested property modification factors for characteristic strength Q and post-yield stiffness K of the LRB. Property modification factors of Table 5 are used to modify the nominal values of Q and K computed by considering the test results presented in Table 2 for 20ºC ambient temperature. Figure 13 presents the corresponding non-deteriorating force-displacement curves used in additional nonlinear response history analyses together with the hysteretic representation for nominal characteristics of the LRB tested in this study.

Table 5 - Property modification factors suggested for -30°C

	λ_Q	λ_K
Constantinou et al. (2007)	1.80	1.30
Li et al. (2009)	1.59	1.30
Imai et al. (2008)	1.57	1.41

The maximum isolator displacements and forces obtained from NRHA performed by using non-deteriorating hysteresis loops ($MID_{non\text{-}deteriorating}$, $MIF_{non\text{-}deteriorating}$) for modeling of LRBs with the ones where deteriorating force-deformation relation ($MID_{deteriorating}$, $MIF_{deteriorating}$) of LRBs was defined based on the experimental data (see Figure 5.b) are compared. Results are illustrated in Figure 14 where grey straight lines represent the case that the response quantities obtained by both non-deteriorating and deteriorating hysteretic representations of LRB are identical to each other. The motivation for evaluation of using property modification factors to estimate the nonlinear response of LRBs at low temperatures (-30°C in this specific case) is to see whether they can be addressed in preliminary design stage of isolated bridges to aid the designer.

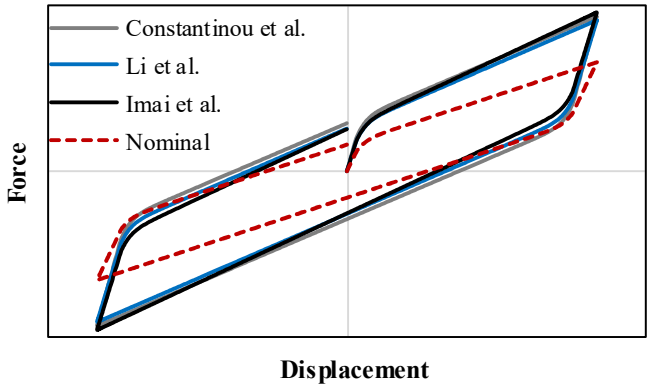

Figure 13 - Force-displacement curves constructed by property modification factors suggested for -30°C.

In Figure 14, in addition to individual results obtained from analyses performed by using each record of ground motion sets (black geometrical forms), their averages are also presented by geometric shapes in red color. In an average sense, Figures 14.a and 14.b demonstrate that using property modification factors of the cited studies is highly effective in estimation of MIDs in comparison to actual deteriorating behavior of LRB. Evaluated property modification factors result in almost the same MIDs for both ground motion sets. For near-field ground motion set, the average MIDs obtained from analysis using property modification factors of Constantinou et al. [7], Li et al. [32] and Imai et al. [45] are 424 mm, 454 mm and 452 mm, respectively while it is 464 mm when the actual deteriorating behavior is used to model isolator response. Average values of MIDs of large-magnitude small-distance ground motion set are 116 mm, 120 mm and 120 mm, in the same order whereas it

is 118 mm for deteriorating hysteretic representation of LRB. In Figure 14.a, it is revealed that for some ground motions, using property modification factors result in under-estimated isolator displacements. In order to assess the reason of such observation, Figure 15 is depicted where force-displacement curves of deteriorating and non-deteriorating (for property modification factors suggested by Constantinou et al. [7]) representations are presented. Figure 15 clearly shows that as the number of large amplitude cycles increases, the corresponding temperature rise in the lead core results in reduced isolator strength for the deteriorating hysteretic representation. Consequently, the isolator experiences amplified displacements. On the other hand, the non-deteriorating hysteretic representation is not sensitive to number of cycles and isolator strength does not change during the cyclic motion. Thus, it is strongly suggested to perform bounding analysis accompanied by the analyses where actual deteriorating force-displacement curve of LRB is taken into account.

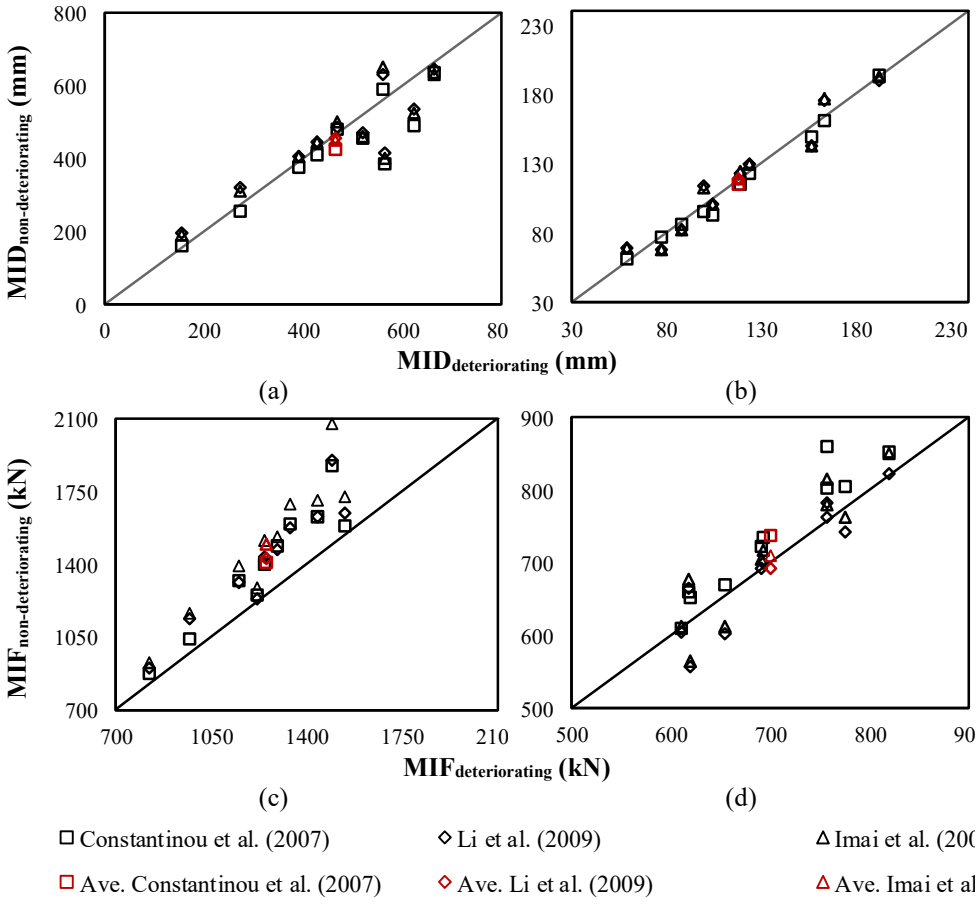

Figure 14 - Accuracy of using property modification factors in prediction of isolator response at -30°C for (a) MID in near-field ground motions, (b) MID in large-magnitude small-distance ground motions, (c) MIF in near-field ground motions, (d) MIF in large-magnitude small-distance ground motions.

Figures 14.c and 14.d show the accuracy of using property modification factors in terms of MIFs. For both ground motion sets, MIFs are over-estimated by non-deteriorating hysteretic representation of LRBs in an average sense. The average amounts of over-estimations range from 10% to 20% for near-field motions while it is less than 5% for large-magnitude small-distance motions. It states that, as the isolator displacement increases, the amount of over-estimation in MIF increases, as well. Thus, the dimensions of bridge piers may be over-sized at the design stage when non-deteriorating representations constructed by property modification factors are used to idealize LRB behavior at an ambient temperature of -30ºC.

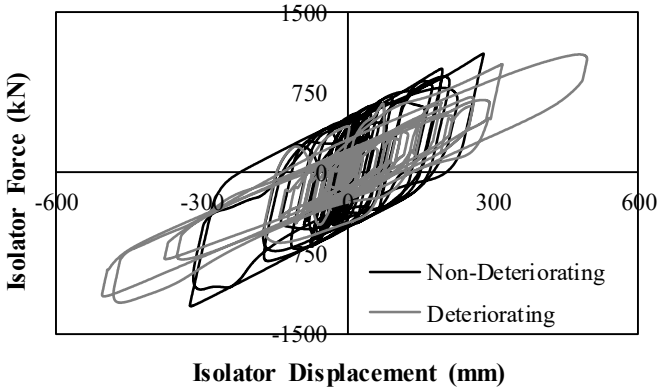

Figure 15 - Comparison of deteriorating and non-deteriorating hysteretic representations for LRB behavior.

9. CONCLUSIONS

This study quantifies the variation in both mechanical properties of an LRB and response of a representative LRB isolated bridge when subjected to bidirectional excitations of ground motions at ambient temperatures of 20°C and -30°C. Hence, a set of complementary experimental and analytical investigations were performed. First, cyclic tests of the considered LRB were conducted and change in hysteretic behavior of the bearing was noted. Then, the recorded hysteretic behavior was compared with the analytically estimated one and the superior ability of the available mathematical model to mimic the force-displacement curve of LRBs under cyclic motion was presented at both ambient temperatures. Using the verified analytical tool for nonlinear behavior of LRB at 20°C and -30°C, nonlinear response history analyses were conducted with two sets of motions representative of both near-field and large-magnitude small-distance records. Results are also used to assess the success of property modification factors in estimation of LRB response at low temperature. Experimental and analytical investigations have revealed the following conclusions:

- Characteristic strength and post-yield stiffness of bilinear force-displacement curve of the tested LRB increases when the temperature drops from 20°C to -30°C. The amplifications in strength and stiffness are observed to be in the order of 50% and 10%, respectively. As the number of cycles increases, these values decrease gradually.

- For the selected ground motions and structural model, in an average sense, MIDs obtained from NRHA conducted with NF motions at -30°C are about 20% less than the ones computed for 20°C. For LMSD motions, it is computed as 16%.
- When the averages of maximum isolator forces obtained from NRHA conducted at -30°C and 20°C were compared, it was found that they are identical for NF motions. On the other hand, average base shear at -30°C is about 30% larger than that of 20°C for LMSD motions.
- Using property modification factors cited in this study results in very accurate estimations for maximum isolator displacement regardless of the ground motion set. However, maximum isolator forces are over-estimated compared to actual deteriorating behavior of LRB. The amount of over-estimation in isolator force increases with increasing isolator displacement. Bounding analysis should be complemented with further analysis where deteriorating hysteretic behavior of LRBs is taken into account.

It is to be mentioned that although the cited studies suggest to use different property modification factors for characteristic strength and post-yield stiffness, they are found to be very effective in estimation of maximum isolator displacement which is the key parameter considered in the design of seismically isolated structures. This observation is important because even though these factors are sensitive to geometry of LRB, manufacturer of the bearing, loading protocol (shear strain and frequency), it is shown that they still provide a good prediction for a randomly selected isolator (different geometry, manufacturer and shear strains). In order to refrain from an over generalization, it should be kept in mind that presented results are specific to both selected ground motions and the tested LRB.

Acknowledgments

This study was supported by research grant No.1505F460, Commission of Scientific Research Projects, Eskisehir Technical University.

References

[1] Skinner, R.I., Robinson, W.H., McVerry, G.H., An Introduction to Seismic Isolation. Chichester: John Wiley & Sons, 1993.

[2] Naeim, F., Kelly J., Design of Seismic Isolated Structures: From Theory to Practice. New York: John Wiley & Sons, 1999.

[3] Kunde, M.C., Jangid, R.S., Seismic Behavior of Isolated Bridges: A-state-of-the-art review. Electronic Journal of Structural Engineering, 3, 140–170, 2003.

[4] Robinson, W.H., Lead Rubber Hysteretic Bearings Suitable for Protecting Structures During Earthquake. Earthquake Engineering and Structural Dynamics, 10(4), 593–604, 1982.

[5] Nagarajaiah, S., Sun, X., Response of Base Isolated USC Hospital Building in Northridge Earthquake. Journal of Structural Engineering (ASCE), 126(10), 1177-1186, 2000.

[6] Roeder, C.W., Proposed Design Method for Thermal Bridge Movements. Journal of Bridge Engineering, 8(1), 12-19, 2003.

[7] Constantinou, M.C., Whittaker, A.S., Kalpakidis, Y., Fenz, D.M., Warn, G.P., Performance of Seismic Isolation Hardware Under Service and Seismic Loading, Technical report, NY: MCEER=07-2012, Buffalo, 2007.

[8] Benzoni, G., Casarotti, C., Effects of Vertical Load, Strain Rate and Cycling on The Response of Lead-Rubber Seismic Isolators. Journal of Earthquake Engineering, 13(3), 293-312, 2009.

[9] Erdoğdu, H., Çavdar, E., Özdemir, G., Türk Deprem Yönetmelikleri (DBYBHY ve TBDY) Spektrum Tanımlarının Deprem Yalıtım Sistemi Tasarımı Özelinde Karşılaştırılması. Teknik Dergi, 32(5), 2021.

[10] Pinarbasi, S., Akyuz, U., Sismik İzolasyon ve Elastomerik Yastik Deneyleri. İMO Teknik Dergi, 237, 3581-3598, 2005.

[11] Roeder, C.W., Stanto, J.F., Taylor A.W., Performance of Elastomeric Bearings (No. 298). Washington, DC: National Cooperative Highway Research Program, Transportation Research Board, 1987.

[12] Ritchie, D.F., Neoprene Bridge Bearing Pads, Gaskets and Seals. Rubber World, Lippincott & Petto Inc. 200(2), 27–31, 1989.

[13] Eyre, R., Stevenson, A., Performance of Elastomeric Bridge Bearings at Low Temperatures. Proceedings 3rd World Congress on Joint Sealing and Bearing Systems for Concrete Structures, 736-762. Toronto, Canada, 1991.

[14] Yakut, A., Yura, J.A., Evaluation of Low-Temperature Test Methods for Elastomeric Bridge Bearings. Journal of Bridge Engineering, 7(1), 50-56, 2002(a).

[15] Yakut, A., Yura. J.A., Parameters Influencing Performance of Elastomeric Bearings at Low Temperatures. Journal of Structural Engineering, 128(8), 986–994., 2002(b).

[16] Fuller, K.N.G., Gough, J., Thomas, A.G., The Effect of Low-Temperature Crystallization on The Mechanical Behavior of Rubber. Journal of Polymer Science: Part B: Polymer Physics, 42(11), 2181-2190, 2004.

[17] Cardone, D., Gesualdi, G., Nigro, D., Effects of Air Temperature on The Cyclic Behavior of Elastomeric Seismic Isolators. Bulletin of Earthquake Engineering, 9(4), 1227–55, 2011.

[18] Hasegawa, O., Shimoda, I., Ikenaga, M., Characteristic of Lead Rubber Bearing by Temperature. Summaries of Technical Papers of Annual Meeting Architectural Institute of Japan, B-2, Structures II, Structural Dynamics Nuclear Power Plants, Architectural Institute of Japan, pp: 511-512, 1997.

[19] Cho, C.B, Kwahk, I.J., Kim, Y. J., An Experimental Study for The Shear Property and The Temperature Dependency of Seismic Isolation Bearings. Journal of the Earthquake Engineering Society of Korea, 12(1), 67-77, 2008.

[20] Park, J.Y., Jang, K.S., Lee, H.P., Lee, Y.H., Kim, H., Experimental Study on The Temperature Dependency of Full-Scale Low Hardness Lead Rubber Bearing. Journal of Computational Structural Engineering, 25(6), 533-540, 2012.

[21] Billah, M., Todorov, B., Effects of Subfreezing Temperature on The Seismic Response of Lead Rubber Bearing Isolated Bridge. Soil Dynamics and Earthquake Engineering, 126, 1-13, 2019.

[22] Deng, P., Gan, Z., Hayashikawa, T., Matsumoto, T., Seismic Response of Highway Viaducts Equipped with Lead-Rubber Bearings Under Low Temperature. Engineering Structures, 209:110008, 2019.

[23] Kalpakidis, I.V., Constantinou, M.C., Whittaker, A.S., Modeling Strength Degradation in Lead–Rubber Bearings Under Earthquake Shaking. Earthquake Engineering and Structural Dynamics, 39(13), 1533–49, 2010.

[24] Ozdemir, G., Avsar, O. Bayhan, B., Change in Response of Bridges Isolated with LRBs Due to Lead Core Heating. Soil Dynamics and Earthquake Engineering, 31(7), 921-929, 2011.

[25] Ozdemir, G., Dicleli, M., Effect of Lead Core Heating on The Seismic Performance of Bridges Isolated with LRB In Near-Fault Zones. Earthquake Engineering and Structural Dynamics, 41(14), 1989-2007, 2012.

[26] Ozdemir, G., Lead Core Heating in LRBs Subjected to Bidirectional Ground Motion Excitations in Various Soil Types. Earthquake Engineering and Structural Dynamics, 43(2), 267-285, 2014.

[27] Kumar, M., Whittaker, A.S., Constantinou, M.C., An Advanced Numerical Model of Elastomeric Seismic Isolation Bearings. Earthquake Engineering and Structural Dynamics, 43(13), 1955–1974, 2014.

[28] Ozdemir, G., Bayhan, B., Gulkan, P., Variations in The Hysteretic Behavior of LRBs as a Function of Applied Loading. Structural Engineering and Mechanics, 67(1), 69-78, 2018.

[29] Wang, H., Zheng, W.Z., Li, J., Gao, Y.Q., Effects of Temperature and Lead Core Heating on Response of Seismically Isolated Bridges Under Near-Fault Excitations. Advances in Structural Engineering, 22(14), 2966-2981, 2019.

[30] Kalpakidis, I.V., Constantinou, M.C., Effects of Heating on The Behavior of Lead-Rubber Bearings. I: Theory. Journal of Structural Engineering, 135(12), 1440–1449, 2009a.

[31] Kalpakidis, I.V., Constantinou, M.C., Effects of Heating on The Behavior of Lead-Rubber Bearings. II: Verification of Theory. Journal of Structural Engineering, 135(12), 1450–1461, 2009b.

[32] Li, J., Ye, K., Jiang, Y.C., Thermal Effect on The Mechanical Behavior of Lead-Rubber Bearing. Journal of Huazhong University of Science and Technology Urban Science, 138(7), 867-876, 2009.

[33] Guay, L.P. and Bouaanani, N., Assessment of low temperature exposure for design and evaluation of elastomeric bridge bearings and seismic isolators in Canada. Canadian Journal of Civil Engineering, 43(9), 851-863, 2016.

[34] ISO (International Organization for Standardization). ISO 22762-1:2005: Elastomeric seismic-protection isolators – Part 1: Test methods, 2005.

[35] OpenSees, Open System for Earthquake Engineering Simulation; Version: 2.1.0, University of California, Pacific Earthquake Engineering Research Center, Berkeley, California, 2001.

[36] Berger/Abam Engineers, Inc. Federal Highway Administration Seismic Design Course, Design Example No.4, 1996. https://ntrl.ntis.gov/NTRL/dashboard/searchResults/titleDetail/PB97142111.xhtml

[37] Warn, G.P., Whittaker, A.S., Performance Estimates in Seismically Isolated Bridge Structures. Engineering Structures, 26(9), 1261–78, 2004.

[38] Dicleli, M., Performance of Seismic-Isolated Bridges in Relation to Near-Fault Ground-Motion and Isolator Characteristics. Earthquake Spectra, 22(4), 887-907, 2006.

[39] Avşar, O., Ozdemir, G., Response of Seismic-Isolated Bridges in Relation to Intensity Measures of Ordinary and Pulselike Ground Motions. Journal of Bridge Engineering, 18(3), 250-260, 2013.

[40] Park, Y.J., Wen, Y.K., Ang, A.H., Random Vibration of Hysteretic Systems Under Bi-Directional Ground Motions. Earthquake Engineering and Structural Dynamics, 14(4), 543-557, 1986.

[41] Mokha, A.S., Constantinou, M.C., Reinhorn, A.M., Verification of Friction Model of Teflon Bearings Under Triaxial Load. Journal of Structural Engineering (ASCE), 119(1), 240-261, 1993.

[42] Pacific Earthquake Engineering Research (PEER) Center. Strong motion data base, 2012. Available from https://ngawest2.berkeley.edu/

[43] QuakeManager, A software framework for ground motion record management selection, analysis and modification; Version:1.80. https://www.eqsols.com/QuakeManager.html

[44] Warn, G.P., Whittaker, A.S., Property Modification Factors for Seismically Isolated Bridges. Journal of Bridge Engineering, 11(3), 371-377, 2006.

[45] Imai, T., Satoh, T., Nishimura, T., Tanaka, H., Mitamura, H., The Performance Evaluations of Rubber Bearings for Bridges in Cold Districts. Proceeding of Hokkaido Chapter of JSCE, p. A-18, 2008.